
Article:
Ruderman, M.S., Petrukhin, N.S. and Kataeva, L.Y. (2025) Nonlinear propagating slow waves in cooling coronal magnetic loops. Solar Physics, 300 (6). 85. ISSN: 0038-0938

https://doi.org/10.1007/s11207-025-02496-y

Solar Physics (2025) 300:85
https://doi.org/10.1007/s11207-025-02496-y

RESEARCH

Nonlinear Propagating Slow Waves in Cooling Coronal Magnetic Loops

M.S. Ruderman[1,2,3] · N.S. Petrukhin[4] · L.Y. Kataeva[5]

Received: 4 April 2025 / Accepted: 29 May 2025

Abstract

We study the propagation of slow magnetosonic waves in coronal magnetic loops. In our study we take nonlinearity and loop cooling into account. We use the small beta approximation and neglect the effect of magnetic field perturbation on the wave propagation. In accordance with this we assume that the tube cross-section does not change. We also neglect the equilibrium plasma density variation along and across the tube. As a result the equations of magnetohydrodynamics reduce to purely one-dimensional gasdynamic equations that includes the effect of viscosity and thermal conduction. We assume that the perturbation amplitude is sufficiently small and use the reductive perturbation method to derive the generalised Burgers' equation describing the evolution of initial perturbations. First we study a case with weak dissipation and drop the term describing it. When there is no cooling the evolution of the initial perturbation results in a gradient catastrophe. However strong cooling can prevent it. Then we solve the full equation numerically assuming that the temperature decreases exponentially. We fix the initial perturbation amplitude and then study the dependence of perturbation evolution on the cooling time. The main result that we obtain is that moderate cooling decelerates the wave damping. This effect is related to the fact that the dissipation coefficients are proportional to the temperature in $5/2$ power. As a result they decrease fast because of plasma cooling. However strong cooling can cause perturbation damping on its own.

Keywords Corona · Coronal magnetic loops · Waves

✉ M.S. Ruderman
m.s.ruderman@sheffield.ac.uk

1 Solar Physics and Space Plasma Research Centre (SP2RC), School of Mathematics and Physics, University of Sheffield, Hicks Building, Hounsfield Road, Sheffield, S3 7RH, UK

2 Space Research Institute (IKI) Russian Academy of Sciences, Moscow, Russia

3 Moscow Center for Fundamental and Applied Mathematics, Lomonosov Moscow State University, Moscow, Russia

4 National Research University Higher School of Economics, Moscow, Russia

5 Nizhny Novgorod State Technical University n.a. Alekseev, Nizhny Novgorod, Russia

Published online: 19 June 2025

1. Introduction

At present it is well known that the solar atmosphere is highly imhomogeneous and dynamic (e.g. Vaiana, Krieger, and Timothy 1973; Schrijver et al. 1999). Observations show that waves and oscillations are always present in the solar atmosphere (e.g. Wang et al. 2003; Okamoto et al. 2007; Jess et al. 2009; Morton et al. 2012; Keys et al. 2018; Jafarzadeh et al. 2024), (see also the reviews by Nakariakov and Verwichte 2005; Zaqarashvili and Erdélyi 2009; Mathioudakis, Jess, and Erdélyi 2013; Wang et al. 2021). In particular the *Ultraviolet Coronagraph Spectrometer* onboard the *Solar Heliospheric Observatory* (SOHO/UVCS) detected propagating disturbances in coronal plumes (Ofman et al. 1997; Ofman, Nakariakov, and Sehgal 2000; Ofman et al. 2000). They were interpreted as slow magnetosonic waves (Ofman, Nakariakov, and DeForest 1999). Later similar disturbances were observed in coronal loops by the *Transition Region and Coronal Explorer* (TRACE) (Nightingale, Aschwanden, and Hurlburd 1999; Schrijver et al. 1999; McEwan and De Moortel 2006). Standing and reflected propagating waves have been observed by the *Soft X-ray Telescope* (SXT) onboard Yohkoh and the *Solar Ultraviolet Measurement Emitted Radiation* (SUMER) spectrum onboard SOHO (Wang et al. 2003; Taroyan et al. 2007) in hot coronal loops.

One important feature that can affect the properties of waves and oscillations in the solar corona is the temperature evolution of coronal plasma. There has been many observations showing that there are various scenarios of temperature evolution (e.g. Winebarger, Warren, and Seaton 2003; Nagata et al. 2003; López Fuentes, Klimchuk, and Mandrini 2007; Aschwanden and Terradas 2008; Viall and Klimchuk 2012; Li et al. 2015). Both kink (Morton and Erdélyi 2009; Ruderman 2011a,b; Ruderman, Shukhobodskiy, and Erdélyi 2017) and sausage (Al-Ghafri and Erdélyi 2013; Al-Ghafri et al. 2014; Al-Ghafri 2015) in cooling coronal loops have been studied in the linear approximation.

Propagation of slow nonlinear waves in coronal loops and plumes has been studied by Nakariakov et al. (2000), Ofman, Nakariakov, and Sehgal (2000), and Ofman et al. (2000). These authors derived the equation describing the spatial evolution of nonlinear waves that takes into account the effects of viscosity, thermal conduction, and gravitational stratification. The analytical results have been compared with the direct numerical modelling. Subsequently standing slow nonlinear waves in coronal loops have also been studied both numerically as well as analytically (Ofman and Wang 2002; Mendoza-Briceño, Erdélyi, and Sigalotti 2004; Sigalotti, Mendoza-Briceño, and Luna-Cardozo 2007; Verwichte et al. 2008; Ruderman 2013).

We aim to study the same problem as that investigated by Al-Ghafri and Erdélyi (2013), however taking the effect of nonlinearity into account. The article is organised as follows: In the next section we describe the equilibrium state and present the governing equations. In Section 3, we derive the equation governing the time dependence of the plasma velocity. In Section 4, we study the joint effect of nonlinearity and equilibrium temperature variation in the approximation of ideal plasma where the effects of viscosity and thermal conduction are neglected. In Section 5, we present the results of numerical solution of the initial value problem for the equation derived in Section 3. Section 6 contains the summary of the results and our conclusions.

2. Equilibrium State and Governing Equations

We study slow propagating waves in hot coronal loops with the temperature $T \gtrsim 6$ MK. In these hot loops the atmospheric scale height exceeds 300 Mm. Hence, we can safely neglect

the density variation along a loop if the height of the loop apex point is smaller than or of the order of 100 Mm. The plasma number density in hot loops is usually not higher than 10^{15} m^{-3}. Then, for $T \leq 10$ MK, the plasma pressure does not exceed 0.23 Nm^{-2}. Using this result we find that the plasma beta is smaller than 0.6 when $B \gtrsim 10^{-3}$ Tesla $= 10$ G. Although this value of plasma beta is not small it is still less than unity. If $B = 20$ G then we obtain plasma beta equal to 0.15, which is much smaller than unity. In accordance with these estimates we use the low-beta plasma approximation and neglect the magnetic field perturbation when studying the slow waves in hot coronal loops. This approximation greatly simplifies the analysis because this enables us to neglect the variation of the loop cross-section and the equilibrium quantities in the directions perpendicular to the loop axis. Neglecting in addition the loop curvature we can describe the slow waves by one-dimensional hydrodynamic equations (Priest 1982; Goedbloed and Poedts 2004)

$$\frac{\partial \rho}{\partial t} + \frac{\partial (\rho u)}{\partial x} = 0, \tag{1}$$

$$\frac{\partial u}{\partial t} + u\frac{\partial u}{\partial x} = -\frac{1}{\rho}\frac{\partial p}{\partial x} + \frac{1}{\rho}\frac{\partial}{\partial x}\rho\nu\frac{\partial u}{\partial x}, \tag{2}$$

$$\frac{\partial T}{\partial t} + u\frac{\partial T}{\partial x} + (\gamma - 1)T\frac{\partial u}{\partial x} = \frac{\partial}{\partial x}\kappa\frac{\partial T}{\partial x} + Q(\rho, T), \tag{3}$$

$$p = \frac{k_B}{m}\rho T. \tag{4}$$

Here u is the velocity, ρ the density, p the pressure, T the temperature, γ the ratio of specific heats, k_B the Boltzmann constant, m the mean mass for particle ($m \approx 0.6 m_{\rm p}$ in the solar corona, where $m_{\rm p}$ is the proton mass), ν the kinematic viscosity, κ the coefficient of thermal conduction, and $Q(\rho, T)$ the generalised heat-loss function. Using the expression for the viscosity tensor and heat flux in a fully ionised plasma given by Braginskii (1965) we obtain

$$\nu = \frac{4\eta_0}{3\rho}, \quad \kappa = \frac{(\gamma - 1)mk_{\parallel}}{\rho k_B}, \tag{5}$$

where η_0 is the first viscosity coefficient in the Braginskii's expression for the viscosity tensor, and $k_{\parallel}$ the thermal conductivity parallel to the magnetic field. The latter two quantities are given by (Braginskii 1965)

$$\eta_0 \approx n k_B T \tau_p, \tag{6}$$

and (e.g. Spitzer 1962; Priest 1982)

$$k_{\parallel} \approx 10^{-11} T^{5/2}\ \mathrm{W\,m^{-1}\,K^{-1}}, \tag{7}$$

where $n = \rho/m_{\rm p}$ is the electron number density and τ_p the proton collision time. It is given by the approximate expression

$$\tau_p \approx 1.66 \times 10^7 \frac{T^{3/2}}{n \ln \Lambda}\ \mathrm{s}, \tag{8}$$

where Λ is the Coulomb logarithm and the number density n is measured in m^{-3}. For typical conditions in hot loops $\ln \Lambda \approx 20$, and τ_p is approximately between 10 and 25 s.

The system of Equations 1 – 4 is the same as was used by Ruderman (2013), and almost the same as was used by Ofman and Wang (2002). The only difference from the latter is that we neglected the term describing the viscous heating in the energy Equation 4. The reason for this is that this term is quadratic with respect to u, while, in what follows, we linearise the dissipative terms. We assume that the unperturbed density is constant, while the unperturbed plasma pressure depends on time and it is proportional to the unperturbed temperature. The assumption that the density does not vary along a hot loop with the temperature of the order of or higher than 6 MK seems reasonable because in this case the atmospheric scale height is much higher than the height of the loop apex. It also seems reasonable to assume that the density does not change with time when the temperature remains high enough, say above 3 or 4 MK. However when it drops below this value the plasma pressure cannot support the almost constant density in the loop. The plasma in the loop starts to flow in the direction of chromosphere. As a result the density will vary along the loop. Hence, although below we consider the temperature decrease about four times the obtained results can be considered reliable only for the temperature decrease of about two times, while the results obtained for lower values of the temperature should be taken with caution.

The assumption that the unperturbed density is constant implies that the unperturbed quantities are related by

$$p_0(t) = \frac{k_B}{m}\rho_0 T_0(t). \tag{9}$$

We also assume that the unperturbed velocity is zero. The variation of the unperturbed temperature is described by

$$\frac{\mathrm{d}T_0}{\mathrm{d}t} = Q(\rho_0, T_0). \tag{10}$$

3. Derivation of the Governing Equation for the Velocity

To derive the governing equation we use the Reductive Perturbation method (Kakutani et al. 1968; Taniuti and Wei 1968). Following Ruderman (2013) we assume that the dissipation is weak and introduce the scaled coefficients $\bar{\nu} = \epsilon^{-1}\nu$ and $\bar{\kappa} = \epsilon^{-1}\kappa$, where $\epsilon \ll 1$. Below we consider either spatially periodic initial perturbations with the period L, or perturbations with finite length L. Then the characteristic time of the problem is L/c_0, where c_0 is the characteristic value of the sound speed. We assume that the characteristic time of variation of the plasma temperature and pressure is $\epsilon^{-1}(L/c_0)$. In accordance with this we introduce the "slow" time $t_1 = \epsilon t$. Hence, p_0 and T_0 are the functions of t_1. We also assume that the oscillation amplitude is relatively small and neglect the effect of perturbations on ν and κ. Then it follows from Equations 5 – 8 that

$$\nu = \nu_0 \left(\frac{T_0(t_1)}{T_{00}}\right)^{5/2}, \quad \eta = \eta_0 \left(\frac{T_0(t_1)}{T_{00}}\right)^{5/2}, \tag{11}$$

where ν_0, η_0, and T_{00} are the values of ν, η, and T_0 at $t = 0$. While the variation of the perturbation shape occurs on the slow time, there is also fast motion described by the "normal" time t, so there are two times, normal and slow. To describe this two-time evolution of the system in geometrical optics all perturbations are taken in the form $w(t_1)\exp(\mathrm{i}\epsilon^{-1}\Theta(t_1))$,

where $\Theta(t_1)$ is eikonal. By analogy with the geometrical optics we introduce

$$X = \epsilon^{-1} \int_0^{t_1} c(t')\,\mathrm{d}t', \quad c^2(t) = \frac{\gamma p_0(t)}{\rho_0}, \tag{12}$$

where $c(t)$ is the unperturbed sound speed. Below we consider waves propagating in the positive x-direction. In accordance with this we assume that perturbations of all variables depend on $\xi = x - X$ and t_1. Using the new variables we transform Equations 1 – 4 to

$$c\frac{\partial \rho}{\partial \xi} - \frac{\partial (\rho u)}{\partial \xi} = \epsilon \frac{\partial \rho}{\partial t_1}, \tag{13}$$

$$c\frac{\partial u}{\partial \xi} - u\frac{\partial u}{\partial \xi} - \frac{1}{\rho}\frac{\partial p}{\partial \xi} = \epsilon \frac{\partial u}{\partial t_1} - \epsilon \bar{\nu}\frac{\partial^2 u}{\partial \xi^2}, \tag{14}$$

$$c\frac{\partial T}{\partial \xi} - u\frac{\partial T}{\partial \xi} - (\gamma - 1)T\frac{\partial u}{\partial \xi} = \epsilon \frac{\partial T}{\partial t_1} - \epsilon \bar{\kappa}\frac{\partial^2 T}{\partial \xi^2}. \tag{15}$$

Equation 4 remains unchanged. When deriving Equation 15 we took $Q(\rho, T) \approx Q(\rho_0, T_0)$, that is we neglected the variation of the generalised heat-loss function related to the density and temperature perturbation. If we take this variation into account then we arrive at the thermal misbalance problem in a cooling plasma. This problem was studied by many authors in a plasma with the constant unperturbed temperature (e.g. Kolotkov, Duckenfield, and Nakariakov 2020; Kolotkov, Zavershinskii, and Nakariakov 2021; Kolotkov and Nakariakov 2022; see also review by Nakariakov et al. 2024). We postpone studying the thermal misbalance problem in a cooling plasma till future research.

We look for the solution to the system of Equations 4 and 13 – 15 in the form of expansions

$$f = f_0 + \epsilon f_1 + \epsilon^2 f_2 + \cdots, \tag{16}$$

where f represents any of quantities u, ρ, p and T. The first term, f_0, corresponds to the unperturbed state. We note that $u_0 = 0$, $\rho_0 = \text{const}$, while p_0 and T_0 are functions of t_1.

3.1. First Order Approximation

Substituting Equation 16 in Equations 4 and 13 – 15 and collecting the terms of the order of ϵ yields

$$c\frac{\partial \rho_1}{\partial \xi} - \rho_0\frac{\partial u_1}{\partial \xi} = 0, \tag{17}$$

$$c\frac{\partial u_1}{\partial \xi} - \frac{1}{\rho_0}\frac{\partial p_1}{\partial \xi} = 0, \tag{18}$$

$$c\frac{\partial T_1}{\partial \xi} - (\gamma - 1)T_0\frac{\partial u_1}{\partial \xi} = 0, \tag{19}$$

$$p_1 = \frac{k_B}{m}(\rho_0 T_1 + T_0 \rho_1). \tag{20}$$

Using Equations 17 – 19 we obtain

$$\rho_1 = \frac{\rho_0}{c} u_1, \quad p_1 = c\rho_0 u_1, \quad T_1 = (\gamma - 1)\frac{T_0}{c} u_1. \tag{21}$$

We note that in accordance with Equation 10 the term $\partial T_0/\partial t_1$ does not appear in Equation 19.

Using the relation $c^2 = \gamma k_B T_0/m$ we can verify that the relations given by Equation 21 satisfy Equation 20.

3.2. Second Order Approximation

In the second order approximation we collect the terms of the order of ϵ^2 in Equations 4 and 13 – 15. Then using Equations 9 and 17 – 19 we obtain

$$c\frac{\partial \rho_2}{\partial \xi} - \rho_0 \frac{\partial u_2}{\partial \xi} = \frac{2\rho_0}{c} u_1 \frac{\partial u_1}{\partial \xi} + \rho_0 \frac{\partial (u_1/c)}{\partial t_1}, \tag{22}$$

$$c\frac{\partial u_2}{\partial \xi} - \frac{1}{\rho_0}\frac{\partial p_2}{\partial \xi} = \frac{\partial u_1}{\partial t_1} - \bar{\nu}\frac{\partial^2 u_1}{\partial \xi^2}, \tag{23}$$

$$c\frac{\partial T_2}{\partial \xi} - (\gamma - 1)T_0 \frac{\partial u_2}{\partial \xi} = (\gamma - 1)\left(\frac{\gamma T_0}{c} u_1 \frac{\partial u_1}{\partial \xi} + \frac{\partial (T_0 u_1/c)}{\partial t_1} - \frac{\bar{\kappa}}{c} T_0 \frac{\partial^2 u_1}{\partial \xi^2}\right), \tag{24}$$

$$p_2 - \frac{k_B}{m}(\rho_0 T_2 + T_0 \rho_2) = \frac{p_0}{c^2}(\gamma - 1)u_1^2. \tag{25}$$

Eliminating u_2, ρ_2, p_2, and T_2 from Equations 22 – 25 we obtain the equation describing the evolution of u_1:

$$2\frac{\partial u_1}{\partial t_1} + (\gamma + 1)u_1 \frac{\partial u_1}{\partial \xi} - \left(\bar{\nu} + \frac{(\gamma - 1)\bar{\kappa}}{\gamma}\right)\frac{\partial^2 u_1}{\partial \xi^2} - \frac{2 - \gamma}{\gamma c}\frac{\mathrm{d}c}{\mathrm{d}t_1} u_1 = 0. \tag{26}$$

Returning to the original variables and using the approximate relation $u \approx \epsilon u_1$ we transform this equation to

$$\frac{\partial u}{\partial t} + c\frac{\partial u}{\partial x} + \frac{\gamma + 1}{2} u \frac{\partial u}{\partial x} - \Gamma \frac{\partial^2 u}{\partial x^2} - \frac{2 - \gamma}{2\gamma c}\frac{\mathrm{d}c}{\mathrm{d}t} u = 0, \tag{27}$$

where

$$\Gamma = \frac{\nu}{2} + \frac{(\gamma - 1)\kappa}{2\gamma}. \tag{28}$$

Below we impose the condition that u either tends to zero as $|x| \to \infty$ sufficiently fast, of it is a periodic function of x. Multiplying Equation 27 by $2u$ and integrating with respect to x we obtain

$$\frac{\mathrm{d}}{\mathrm{d}t} c^{1-2/\gamma} \int u^2 \,\mathrm{d}x = -2\Gamma c^{1-2/\gamma} \int \left(\frac{\partial u}{\partial x}\right)^2 \mathrm{d}x, \tag{29}$$

where the integrals are taken either over the interval $(-\infty, \infty)$ or over the period of u with respect to x. When $\Gamma = 0$ we obtain

$$c^{1-2/\gamma} \int u^2 \, \mathrm{d}x = \text{const.} \tag{30}$$

Since the equilibrium quantities vary with time the energy of perturbation is not conserved. However when $\Gamma = 0$ the energy variation is only due to changing of the equilibrium quantities, while when $\Gamma \neq 0$ the energy also decreases due to the energy dissipation. Hence, Equation 30 can be considered as the modified energy conservation law.

We impose the initial condition

$$u = \phi(x) \quad \text{at } t = 0. \tag{31}$$

4. Solution for Weak Dissipation

In this section we consider the case of weak dissipation. We start the analysis with introducing the dimensionless variables:

$$y = \frac{1}{L}\left(x - \int_0^t c(t')\,\mathrm{d}t'\right), \quad \tau = \frac{u_0 t}{L}, \quad U = \frac{u}{u_0}, \quad C = \frac{c}{c_0}, \quad R = \frac{u_0 L}{\Gamma_0}, \tag{32}$$

where $c_0 = c(0)$, $\Gamma_0 = \Gamma(0)$, L is the characteristic spatial length, and u_0 is the characteristic value of u. For example we can take u_0 equal to the maximum value of $|u|$. In these variables Equation 27 is transformed to

$$\frac{\partial U}{\partial \tau} + \frac{1}{2}(\gamma+1)U\frac{\partial U}{\partial y} - \frac{C^5}{R}\frac{\partial^2 U}{\partial y^2} - \frac{2-\gamma}{2\gamma C}\frac{\mathrm{d}C}{\mathrm{d}\tau}U = 0. \tag{33}$$

When deriving this equation we used Equation 5 and the relation $T_0/T_{00} = c^2/c_0^2$. Weak dissipation corresponds to $R \gg 1$. In this case we can neglect the third term in Equation 33 and reduce it to

$$\frac{\partial U}{\partial \tau} + \frac{1}{2}(\gamma+1)U\frac{\partial U}{\partial y} - \frac{2-\gamma}{2\gamma C}\frac{\mathrm{d}C}{\mathrm{d}\tau}U = 0. \tag{34}$$

The equation of characteristics of this equation is defined by

$$\frac{\mathrm{d}y}{\mathrm{d}\tau} = \frac{\gamma+1}{2}U. \tag{35}$$

Let $y = y(\tau)$ be the equation of a characteristic. On this characteristic $U = U(\tau, y(\tau))$. Then the variation of U along this characteristic is described by

$$\frac{\mathrm{d}U}{\mathrm{d}\tau} = \frac{2-\gamma}{2\gamma C}\frac{\mathrm{d}C}{\mathrm{d}\tau}U. \tag{36}$$

The solution to this equation is

$$U(\tau, y(\tau)) = U_0 C^{\frac{2-\gamma}{2\gamma}}, \tag{37}$$

where U_0 is the value of U at $\tau = 0$. The initial condition given by Equation 31 is transformed in the dimensionless variables to

$$U(\tau, y(\tau)) = \frac{\phi(x)}{u_0} \equiv \Phi(y(\tau)) \quad \text{at } \tau = 0. \tag{38}$$

It follows from Equations 37 and 38 that $U_0 = \Phi(y_0)$, where $y_0 = y(0)$. Using this result we transform Equation 37 to

$$U(\tau, y(\tau)) = \Phi(y_0)[C(\tau)]^{\frac{2-\gamma}{2\gamma}}. \tag{39}$$

Substituting this result in Equation 35 we obtain that the equation of the characteristic satisfying $y_0 = y(0)$ is

$$\frac{\mathrm{d}y}{\mathrm{d}\tau} = \frac{\gamma+1}{2}\Phi(y_0)[C(\tau)]^{\frac{2-\gamma}{2\gamma}}. \tag{40}$$

Integrating this equation we obtain that the equation of this characteristic is

$$y = y_0 + \frac{\gamma+1}{2}\Phi(y_0)\int_0^\tau [C(\tau')]^{\frac{2-\gamma}{2\gamma}}\,\mathrm{d}\tau'. \tag{41}$$

To calculate the value of U at point (τ, y) we must find such a value of y_0 that the characteristic starting at y_0 contains this point. As a result we obtain $y_0(\tau, y)$. Substituting this function in Equation 39 we obtain

$$U(\tau, y) = \Phi(y_0(\tau, y))[C(\tau)]^{\frac{2-\gamma}{2\gamma}}. \tag{42}$$

However this expression can be only obtained if Equation 41 determines y_0 as a single-valued function of τ and y. The derivative of the right-hand side of Equation 41 with respect to y_0 is

$$D(\tau, y_0) = 1 + \frac{\gamma+1}{2}\frac{\mathrm{d}\Phi(y_0)}{\mathrm{d}y_0}\int_0^\tau [C(\tau')]^{\frac{2-\gamma}{2\gamma}}\,\mathrm{d}\tau'. \tag{43}$$

We see that $D(0, y_0) = 1 > 0$. Then there are two possibilities. If $D(\tau, y_0) > 0$ for any $\tau > 0$ then there is the single-valued solution to Equation 41 determining $y_0(\tau, y)$ and, consequently, there is the solution to the initial value problem to Equation 33 given by Equation 42 for $\tau > 0$.

However, when $D(\tau, y_0) > 0$ only for $\tau < \tau_c$ while $D(\tau_c, y_0) = 0$, then there is the single-valued solution to Equation 41 determining $y_0(\tau, y)$ only for $\tau < \tau_c$ and, consequently, there is the solution to the initial value problem to Equation 33 given by Equation 42 only for $\tau < \tau_c$. Differentiating Equation 41 yields

$$\frac{\partial y_0}{\partial y} = \frac{1}{D(\tau, y_0)}. \tag{44}$$

Using this result we obtain

$$\frac{\partial U}{\partial y} = [C(\tau)]^{\frac{2-\gamma}{2\gamma}}\frac{1}{D(\tau, y_0)}\frac{\mathrm{d}\Phi(y_0)}{\mathrm{d}y_0}. \tag{45}$$

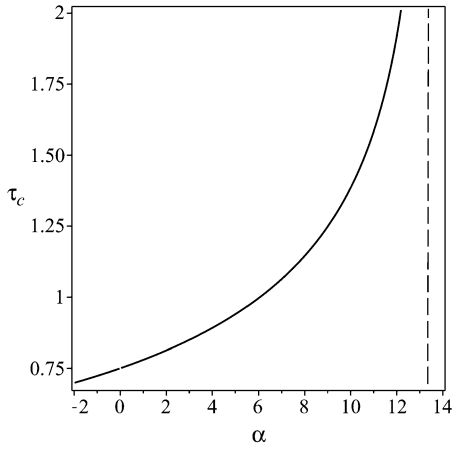

Figure 1 Dependence of τ_c on α. The vertical dashed line shows the value of $\alpha_c = 40/3$.

It follows from this equation that $|\partial U/\partial y| \to \infty$ as $\tau \to \tau_c$. This phenomenon is called a gradient catastrophe that is previously studied, for example, in nonlinear acoustics (e.g. Rudenko and Soluyan 2001), hydrodynamics (e.g. Landau and Lifshitz 1987; Ruderman 2019), and in the general theory of waves (e.g. Whitham 1974). It particular, it was shown that at $\tau = \tau_c$ a shock in the perturbation starts to form.

To give an example we take

$$\Phi(y) = \begin{cases} 0, & y < 0, \\ \sin y, & 0 \le y \le \pi, \\ 0, & y > \pi, \end{cases} \tag{46}$$

$$C(\tau) = \mathrm{e}^{-\alpha\tau}. \tag{47}$$

This sound speed variation corresponds to the temperature varying as $\mathrm{e}^{-2\alpha\tau}$. Positive values of α correspond to cooling of the coronal loop plasma, and negative values to heating. Substituting Equations 46 and 47 into Equation 43 yields

$$D(\tau, y_0) = 1 + \frac{\gamma(\gamma+1)}{\alpha(2-\gamma)}\left(1 - \mathrm{e}^{-\frac{2-\gamma}{2\gamma}\alpha\tau}\right)\cos y_0. \tag{48}$$

This expression is valid for $0 \le y \le \pi$. It is straightforward to see that the sign of the second term on the right-hand side of Equation 48 coincides with the sign of $\cos y_0$. Then it follows that the second term takes minimum when $y_0 = \pi$. After that we immediately find that

$$\tau_c = -\frac{2\gamma}{\alpha(2-\gamma)}\ln\left(1 - \frac{\alpha}{\alpha_c}\right), \quad \alpha_c = \frac{\gamma(\gamma+1)}{2-\gamma}. \tag{49}$$

It is proved in Appendix A that τ_c is a monotonically increasing function of α. When $\alpha \to \alpha_c$ we have $\tau_c \to \infty$. The dependence of τ_c on α is shown in Figure 1. For $\alpha > \alpha_c$ we obtain $D(\tau, y_0) > 0$ for any $\tau > 0$ and the gradient catastrophe does not occur. Hence, we see that sufficiently strong cooling can prevent the gradient catastrophe. However for this cooling must be very strong since $\alpha_c = 40/3$ for $\gamma = 5/3$. The result that strong cooling can prevent the gradient catastrophe has a simple explanation. If we neglect nonlinearity then the shape of perturbation does not change and the solution has the form $U = A(\tau)\Phi(y)$. Substituting

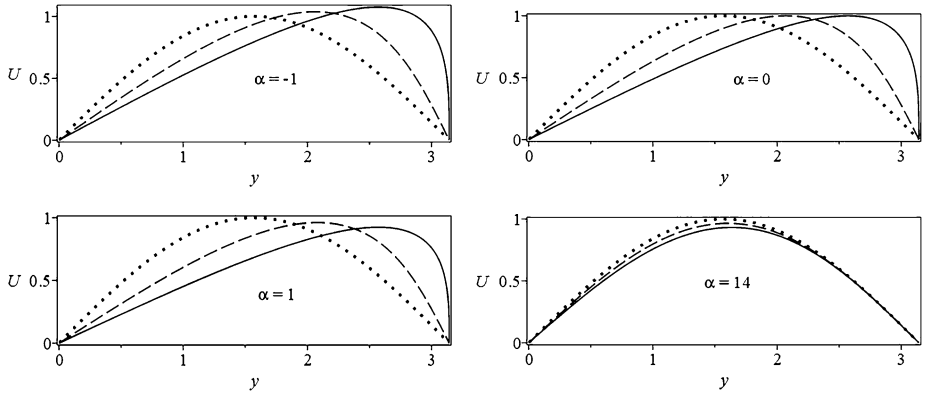

Figure 2 Dependence of U on y for various values of α. In the upper panes as well as in the left lower panel the dotted, dashed, and solid lines correspond to $\tau = 0$, $\tau = \tau_c/2$, and $\tau = \tau_c$. In the right lower panel the dotted, dashed, and solid lines correspond to $\tau = 0$, $\tau = 0.025$, and $\tau = 0.05$.

this expression and Equation 47 into Equation 30 transformed to the dimensionless variables yields

$$A(\tau) = \mathrm{e}^{-\frac{2-\gamma}{2\gamma}\alpha\tau}. \tag{50}$$

We see that the perturbation amplitude decreases when $\alpha > 0$. When cooling is strong the amplitude attenuation prevents the gradient catastrophe.

Using Equation 47 we obtain from Equations 41 and 42

$$y = y_0 + \frac{\gamma(\gamma+1)}{\alpha(2-\gamma)}\Phi(y_0)\left(1 - \mathrm{e}^{-\frac{2-\gamma}{2\gamma}\alpha\tau}\right), \tag{51}$$

$$U(\tau, y) = \Phi(y_0(\tau, y))\mathrm{e}^{-\frac{2-\gamma}{2\gamma}\alpha\tau}. \tag{52}$$

We consider Equations 51 and 52 for $\tau < \tau_c$. It follows from Equation 46 that $y_0 = y$ is a solution to Equation 51 when $y \le 0$ and $y \ge \pi$ for any τ. Since for $\tau < \tau_c$ the solution to Equation 51 for given y and τ is unique it follows that there are no other solutions to Equation 51 for $y \le 0$ and $y \ge \pi$. Then it follows from Equation 52 that $U = 0$ for $y \le 0$ and $y \ge \pi$. Equation 51 was solved numerically and the solution was substituted into Equation 52.

The evolution of U with time is shown in Figure 2 for various values of α. In this figure the evolution of the perturbation is shown up to the instance of gradient catastrophe for the cases when the temperature increases ($\alpha = -1$), the temperature does not change ($\alpha = 0$), and the temperature decreases ($\alpha = 1$). Since $\alpha_c < 14$ the right lower panel in Figure 2 corresponds to the case where the gradient catastrophe does not occur. Since $\tau_c \approx 0.72$ for $\alpha = -1$ and $\tau_c \approx 0.78$ for $\alpha = 1$ the loop temperature increases approximately four times in the first case and decreases approximately five times in the second case when τ varies from 0 to τ_c. In accordance with this estimate we chose to show the evolution of U for τ varying from 0 to 0.05 because the loop temperature decreases approximately four times for $\alpha = 14$ and $\tau = 0.05$.

We can see in Figure 2 that the loop heating causes the increase of the perturbation amplitude, while the loop cooling causes its decrease. However the effect is very weak.

Now we discuss the results obtained in this section using the dimensional variables. The temperature in a cooling coronal loop is given by

$$T_0(t) = T_{00}\mathrm{e}^{-t/t_{\mathrm{cool}}}, \quad t_{\mathrm{cool}} = \frac{L}{2|\alpha|u_0}. \tag{53}$$

Taking $T_{00} = 6$ MK yields $c_0 \approx 370$ km s^{-1}. Next we take $L = 40$ Mm $= 4 \times 10^7$ m and the amplitude of the initial velocity perturbation equal to 10% of the sound speed, that is $u_0 = 37$ km s^{-1}. Then we obtain $t_{\mathrm{cool}} \approx (540/|\alpha|)$ s. This gives $t_{\mathrm{cool}} \approx 540$ s for $|\alpha| = 1$, which is a sufficiently realistic value of cooling time. On the other hand, $t_{\mathrm{cool}} \approx 38.6$ s for $\alpha = 14$, so the cooling time needed to prevent the gradient catastrophe for $u_0 = 37$ km s^{-1} is unrealistically small. To obtain $t_{\mathrm{cool}} = 500$ s for $\alpha = 14$ we must take an extremely small value of $u_0 \approx 2.86$ km s^{-1}, which is about 0.77% of the initial sound speed. It is not surprising that for such a small velocity amplitude the nonlinearity does not affect the wave evolutions as is seen in the bottom right panel in Figure 2.

Introducing $t_c = L\tau_c/u_0$ we obtain that it is equal to 782 s for $\alpha = -1$, to 811 s for $\alpha = 0$, and to 843 s for $\alpha = 1$. We take $\tau = 0.05$ for $\alpha = 14$ that corresponds to 700 s. The loop temperature increases by more than 4 times for $t_c = 782$ s corresponding to $\alpha = -1$, and decreases by almost 5 times for $t_c = 843$ s corresponding to $\alpha = 1$.

We can see from our analysis that cooling alone cannot cause substantial decrease of nonlinear perturbations. Strong damping will only start after the formation of a shock in the wave profile that occurs at $\tau = \tau_c$. However, before that happens viscosity and thermal conduction will start to work. This scenario is studied in the next section.

5. Numerical Solution of Equation 33

Substituting Equation 47 into Equation 33 yields

$$\frac{\partial U}{\partial \tau} + \frac{1}{2}(\gamma+1)U\frac{\partial U}{\partial y} + \frac{\mathrm{e}^{-5\alpha\tau}}{R}\frac{\partial^2 U}{\partial y^2} + \frac{\alpha(2-\gamma)}{2\gamma}U = 0. \tag{54}$$

The initial value problem was solved numerically with the initial condition given by Equation 46. In our numerical study we used $\gamma = 5/3$.

We use the same representative values of parameters as in the previous section. However while in the previous section we had only one parameter, α, now we have the second parameter, R, and we need to choose realistic values for this parameter. For this we need to estimate the value of Γ_0. It follows from the definition of Γ that $\Gamma_0 = 0.5\nu_0 + 0.2\kappa_0$. Taking $T_{00} = 6$ MK and $n_0 = 10^{15}$ m^{-3} we obtain $\nu_0 \approx 8 \times 10^{11}$ m^2 s^{-1} and $\kappa_0 \approx 2.55 \times 10^{13}$ m^2 s^{-1}. Using these numbers yields $\Gamma_0 \approx 5.4 \times 10^{12}$. Then we obtain $R \approx 0.274$. We only consider the effect of cooling and take $\alpha = 1$ and 14. To display the effect of cooling we also consider $\alpha = 0$.

The results of numerical solution of Equation 54 are presented in Figure 3. The upper panel corresponds to the case when there is no cooling. We see that the initial perturbation damps due to viscosity and thermal conduction while there is almost no nonlinear distortion of the perturbation profile. It is not surprising because $R \approx 0.274 \ll 1$ and dissipation substantially dominates nonlinearity. We also notice the diffusion of perturbation beyond the interval $[0, L]$ caused by dissipation.

The middle panel corresponds to the case when there is cooling. We can see that the evolution of the initial perturbation shown in this panel is quite different from that shown

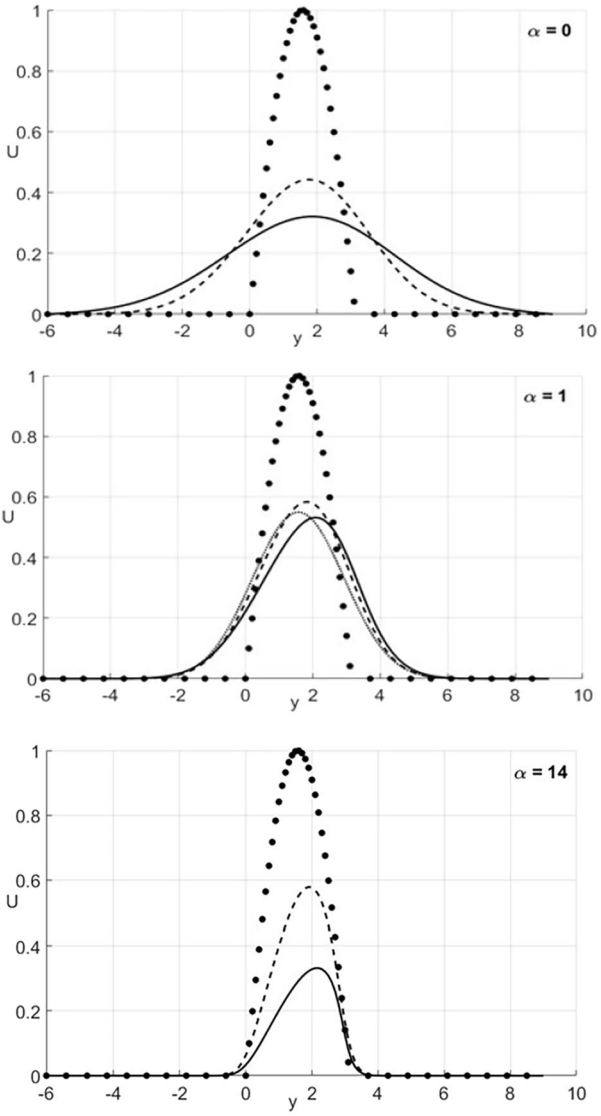

Figure 3 Dependence of U on y for various values of α obtained by solving Equation 54. In the upper and middle panels the dotted, dashed, and solid lines correspond to $\tau = 0$, $\tau = \tau_c/2$, and $\tau = \tau_c$. In the lower panel the dotted, dashed, and solid lines correspond to $\tau = 0$, $\tau = 0.375$, and $\tau = 0.75$. The small-dotted line in the middle panel shows the solution to the linearised Equation 68 for $\tau = \tau_c$.

in the upper panel. Hence we conclude that the effect of cooling is sufficiently strong. The main reason for this is that the coefficient at the third term in Equation 54 decreases with time due to cooling. It decreases almost 50 times at $\tau = \tau_c$ in comparison with its initial value. As a result cooling decelerates the wave damping. We also see that there is some nonlinear distortion of the perturbation profile. To make this even more clear we plot the profile calculated using the solution to the linear problem given by Equation 68. We observe that the solid curve is different from the small-dotted curve. In contrast, a similar comparison for the upper panel does not show practically any difference between the results obtained using linear and nonlinear description. We again notice the diffusion of perturbation beyond the interval $[0, L]$.

Finally, we discuss the results presented in the lower panel in Figure 3. As we have already pointed out in the previous section the cooling time corresponding to the values of L, T_0, and u_0 taken in our calculations is completely unrealistic for $\alpha = 14$. Hence, the results obtained in this case are only interesting from the theoretical point of view, but cannot be applied for interpretation of observational results. The coefficient at the third term describing dissipation is decreasing very fast, so the third term can be neglected. This conclusion is also supported by the fact that the perturbation almost does not diffuse beyond the interval $[0, L]$. We see that there is some nonlinear distortion of the perturbation profile. If we also neglect the nonlinear term and only keep the first and last terms in Equation 54 then the solution to the reduced equation is $U = U_0 \exp(-(\alpha\tau(1/\gamma - 1/2))$. Although this solution does not account for the nonlinear distortion, it sufficiently accurately describes the amplitude variation with the time. Hence, the decrease of the wave amplitude observed in the lower panel in Figure 3 is almost solely due to cooling.

The main conclusion that we can make on the bases of the numerical results presented in the upper and middle panels in Figure 3 is that moderate cooling decelerates the wave dumping due to viscosity and thermal conduction. However, the result obtained for $\alpha = 14$ shows that strong cooling can cause the wave damping on its own.

6. Summary and Conclusions

In this article we studied nonlinear propagating slow sausage waves in a cooling coronal magnetic loop. We used the simplest model of a coronal loop as a straight magnetic tube with a circular cross-section. We also used the cold plasma approximation and neglected the density variation in the tube. As a result the problem reduced to studying propagation of sound waves in a cooling plasma. Using the reductive perturbation method we derived the equation governing the time evolution of the perturbation velocity. When there is no cooling this equation is Burgers' equation. Hence the governing equation can be called the modified Burgers' equation. We then introduced dimensionless variables. In these variables the governing equation, which is Equation 33, contains only one dimensionless parameter, R, and one arbitrary function, $C(\tau)$, related to the temperature dependence on time. Parameter R determines the relative importance of nonlinearity and dissipation. When $R \ll 1$ we can neglect the effect of nonlinearity and use the linear approximation. On the other hand, when $R \gg 1$ we can neglect dissipation.

We solved the modified Burgers' equation for a particular perturbation given by Equation 46 assuming that the temperature decreases exponentially. This problem contains the second dimensionless parameter α. This parameter is defined as $\alpha = L/u_0 t_{\rm cool}$, where L is the length of initially perturbed region, u_0 the amplitude of the initial perturbation, and $t_{\rm cool}$ the cooling time, which is the time during which the temperature decreases e-times. We also considered the coronal loop heating corresponding to $\alpha < 0$.

First we assumed that $R \gg 1$ and neglected the third term in Equation 54. The most important result that we obtained is that for moderate values of α the nonlinear evolution of the initial perturbation results in a gradient catastrophe. However, when $\alpha > \alpha_c$, where $\alpha_c = 40/3$ for $\gamma = 5/3$, a gradient catastrophe does not occur. The condition $\alpha > \alpha_c$ can be written as $t_{\rm cool} < L/\alpha_c u_0$. We see that a sufficiently strong cooling with small cooling time prevents the gradient catastrophe for any fixed perturbation length L and the initial perturbation amplitude u_0. An inspection of Figure 2 shows that cooling reduces the oscillation amplitude, but this effect is quite weak.

Next we considered the case where $R \lesssim 1$ and solved Equation 54 with the same initial condition given by Equation 46. We took typical values of dissipative coefficients at the initial time, so Γ_0 was fixed. We also fixed L and u_0, so R was fixed and approximately equal to 0.274. Hence the only variable dimensional quantity was the cooling time $t_{\rm cool}$. In accordance with Equation 53 $t_{\rm cool}$ is proportional to α^{-1}. We obtained quite realistic value of $t_{\rm cool}$ for $\alpha = 1$ and unrealistically small value for $\alpha = 14$. First effect related to the account of dissipation is the perturbation damping. Next, dissipation causes diffusion of perturbation beyond the initially perturbed interval $[0, L]$. We compared the results obtained by solving Equation 54 with those obtained using the linear approximation. The results practically coincide for $\alpha = 0$, which is not surprising taking into account that R is quite small. The real difference between the results given by linear and nonlinear theories is seen for $\alpha = 1$. This result is related to the fact that the coefficient at the term in Equation 54 describing dissipation decreases due to cooling. In particular, it decreases by about 50 times during the evolution time of the perturbation. When $\alpha = 0$ there is no cooling and the perturbation amplitude decreases by about three times during the evolution time. However, when $\alpha = 1$ it decreases by less than 2 times. Hence, the main effect of cooling is the reduction of perturbation damping. This effect is the direct consequence of the fact that the dissipation coefficients are proportional to $T^{5/2}$, where T is the temperature. However, this is only valid for moderate strength of cooling. The result obtained for $\alpha = 14$ shows that strong cooling can cause the wave damping on its own.

Appendix A: Prove that τ_c is a Monotonically Increasing Function of α

We rewrite Equation 49 as

$$\tau_c = -\frac{2}{x(\gamma+1)}\ln(1-x), \quad x = \frac{\alpha}{\alpha_c}. \tag{55}$$

Differentiating this expression we obtain

$$\frac{{\rm d}\tau_c}{{\rm d}x} = \frac{g(x)}{(\gamma+1)x^2}, \quad g(x) = 2\ln(1-x) + \frac{2x}{1-x}. \tag{56}$$

Next we obtain

$$\frac{{\rm d}g}{{\rm d}x} = \frac{2x}{(1-x)^2}. \tag{57}$$

We see that ${\rm d}g/{\rm d}x < 0$ for $x < 0$ and ${\rm d}g/{\rm d}x > 0$ for $x > 0$. This implies that $g(x)$ takes minimum at $x = 0$. Since $g(0) = 0$ it follows that $g(x) > 0$ for $x \neq 0$. This result implies that τ_c is a monotonically increasing function of x.

Appendix B: Solution of Initial Value Problem to Linearised Equation 33

In this section we assume that $R \ll 1$. In this case we can neglect the second term on the left-hand side of Equation 33 in comparison with the third term and obtain the linear equation that reads

$$\frac{\partial U}{\partial \tau} - \frac{C^5}{R}\frac{\partial^2 U}{\partial y^2} - \frac{2-\gamma}{2\gamma C}\frac{{\rm d}C}{{\rm d}\tau}U = 0. \tag{58}$$

Using the variable substitution

$$U = C^{\frac{2-\gamma}{2\gamma}} W, \quad \theta = \int_0^\tau C^5(\tau')\,\mathrm{d}\tau', \tag{59}$$

we reduce Equation 58 to

$$\frac{\partial W}{\partial \theta} = \frac{1}{R}\frac{\partial^2 W}{\partial y^2}. \tag{60}$$

We impose the initial condition

$$W = W_0(y) \quad \text{at } \theta = 0. \tag{61}$$

The solution to Equation 59 subjected to this initial condition is given by (Polyanin 2002)

$$W(\theta, y) = \frac{1}{2}\sqrt{\frac{R}{\pi\theta}} \int_{-\infty}^{\infty} W_0(z) \exp\left(-\frac{(y-z)^2 R}{4\theta}\right) \mathrm{d}z. \tag{62}$$

First we take $W_0(y) = \sin y$. Then after some algebra we obtain

$$\int_{-\infty}^{\infty} W_0(z) \exp\left(-\frac{(y-z)^2 R}{4\theta}\right) \mathrm{d}z = 2\sin y \int_0^{\infty} \cos z \exp\left(-\frac{z^2 R}{4\theta}\right) \mathrm{d}z. \tag{63}$$

Then using the relation (Prudnikov, Brychkov, and Marichev 1992)

$$\int_0^{\infty} \mathrm{e}^{-ax^2} \cos(bx)\,\mathrm{d}x = \sqrt{\frac{\pi}{4a}}\mathrm{e}^{-b^2/4a} \tag{64}$$

we obtain

$$W(\theta, y) = \mathrm{e}^{-\theta/R} \sin y. \tag{65}$$

Now we use the expression for $C(\tau)$ given by Equation 47 to obtain

$$\theta = \frac{1 - \mathrm{e}^{-5\alpha\tau}}{5\alpha}. \tag{66}$$

Using this result we obtain from Equations 59 and 65

$$U(\tau, y) = A(\tau)\sin y, \quad A(\tau) = \exp\left(-\frac{2-\gamma}{2\gamma}\alpha\tau - \frac{1-\mathrm{e}^{-5\alpha\tau}}{5\alpha R}\right). \tag{67}$$

When $\tau \to \infty$ the temperature tends to zero that does not make any physical sense. Hence, we take $\tau \leq 0.8\alpha^{-1}$ since the temperature decreases $\mathrm{e}^2 \approx 5$ times at $\tau = 0.8\alpha^{-1}$. Depending on the values of α cooling can either accelerate or decelerate the wave damping. However if we take $\gamma = 5/3$ and $R = 0.274$ as in Section 5 then we obtain $A(0.8\alpha^{-1}) \approx 0.067$ for $\alpha = 0$, while $A(0.8\alpha^{-1}) \approx 0.47$ for $\alpha = 1$. We see that in this case cooling strongly decelerates the wave damping. This effect is related to strong decrease of the coefficient at the second term in Equation 58 due to cooling. This term at $\tau = 0.8\alpha^{-1}$ is approximately 50 times smaller than that at $\tau = 0$.

Now we take $W_0(y) = \Phi(y)$, where $\Phi(y)$ is given by Equation 46. We also assume that $C(\tau)$ is given by Equation 47. Then we obtain

$$U(\tau, y) = \frac{1}{2} \mathrm{e}^{-\frac{2-\gamma}{2\gamma}\alpha\tau} \sqrt{\frac{R}{\pi\theta}} \int_0^\pi \sin z \exp\left(-\frac{(y-z)^2 R}{4\theta}\right) \mathrm{d}z, \tag{68}$$

where $\theta(\tau)$ is defined by Equation 66.

Author Contributions The authors made equal contribution.

Data Availability No datasets were generated or analysed during the current study.

Declarations

Competing Interests The authors declare no competing interests.

References

Al-Ghafri, K.S.: 2015, Standing slow MHD waves in radiatively cooling coronal loops. *J. Astrophys. Astron.* **36**, 325. DOI. ADS.

Al-Ghafri, K.S., Erdélyi, R.: 2013, Effect of variable background on an oscillating hot coronal loop. *Sol. Phys.* **283**, 413. DOI. ADS.

Al-Ghafri, K.S., Ruderman, M.S., Williamson, A., Erdélyi, R.: 2014, Longitudinal magnetohydrodynamics oscillations in dissipative, cooling coronal loops. *Astrophys. J.* **786**, 36. DOI. ADS.

Aschwanden, M.J., Terradas, J.: 2008, The effect of radiative cooling on coronal loop oscillations. *Astrophys. J. Lett.* **686**, L127. DOI. ADS.

Braginskii, S.I.: 1965, *Transport processes in plasma, Reviews of Plasma Physics*. Leotovich, M.A. (ed.): **1**, Consultants Bureau, New York, 205.

Goedbloed, J.P.H., Poedts, S.: 2004, *Principles of Magnetohydrodynamics*, Cambridge University Press, Cambridge.

Jafarzadeh, S., Schiavo, L.A.C.A., Fedun, V., Solanki, S.K., Stangalini, M., Calchetti, D., Verth, G., Jess, D.B., Grant, S.D.T., Ballai, I., Gafeira, R., Keys, P.H., Fleck, B., Morton, R.J., Browning, P.K., Silva, S.S.A., Appourchaux, T., Gandorfer, A., Gizon, L., Hirzberger, J., Kahil, F., Orozco Suárez, D., Schou, J., Strecker, H., del Toro Iniesta, J.C., Valori, G., Volkmer, R., Woch, J.: 2024, Sausage, kink, and fluting magnetohydrodynamic wave modes identified in solar magnetic pores by Solar Orbiter/PHI. *Astron. Astrophys.* **688**, A2. DOI. ADS.

Jess, D.B., Mathioudakis, M., Erdélyi, R., Crockett, P.J., Keenan, F.P., Christian, D.J.: 2009, Alfvén waves in the lower solar atmosphere. *Science* **323**, 1582. DOI. ADS.

Kakutani, T., Ono, H., Taniuti, T., Wei, C.-C.: 1968, Reductive perturbation method in nonlinear wave propagation II. Application to hydromagnetic waves in cold plasma. *J. Phys. Soc. Jpn.* **24**, 1159. DOI. ADS.

Keys, P.H., Morton, R.J., Jess, D.B., Verth, G., Grant, S.D.T., Mathioudakis, M., Mackay, D.H., Doyle, J.G., Christian, D.J., Keenan, F.P., Erdélyi, R.: 2018, Photospheric observations of surface and body modes in solar magnetic pores. *Astrophys. J.* **857**, 28. DOI. ADS.

Kolotkov, D.Y., Duckenfield, T.J., Nakariakov, V.M.: 2020, Seismological constraints on the solar coronal heating function. *Astron. Astrophys.* **644**, A33. DOI. ADS.

Kolotkov, D.Y., Nakariakov, V.M.: 2022, A new look at the frequency-dependent damping of slow-mode waves in the solar corona. *Mon. Not. R. Astron. Soc.* **514**, L51. DOI. ADS.

Kolotkov, D.Y., Zavershinskii, D., Nakariakov, V.M.: 2021, The solar corona as an active medium for magnetoacoustic waves. *Plasma Phys. Control. Fusion* **63**, 124008. DOI. ADS.

Landau, L.D., Lifshitz, E.M.: 1987, *Fluid Mechanics, Course of Theoretical Physics* **6**, Pergamon Press, Oxford.

Li, L.P., Peter, H., Chen, F., Zhang, J.: 2015, Heating and cooling of coronal loops observed by SDO. *Astron. Astrophys.* **583**, A109. DOI. ADS.

López Fuentes, M.C., Klimchuk, J.A., Mandrini, C.H.: 2007, The temporal evolution of coronal loops observed by GOES SXI. *Astrophys. J.* **657**, 1127. DOI. ADS.

Mathioudakis, M., Jess, D.B., Erdélyi, R.: 2013, Alfvén waves in the solar atmosphere. From theory to observations. *Space Sci. Rev.* **175**, 1. DOI. ADS.

McEwan, M.P., De Moortel, I.: 2006, Longitudinal intensity oscillations observed with TRACE: evidence of fine-scale structure. *Astron. Astrophys.* **448**, 763. DOI. ADS.

Mendoza-Briceño, C.A., Erdélyi, R., Sigalotti, L.D.G.: 2004, The effects of stratification on oscillating coronal loops. *Astrophys. J.* **605**, 493. DOI. ADS.

Morton, R.J., Erdélyi, R.: 2009, Transverse oscillations of a cooling coronal loop. *Astrophys. J.* **707**, 750. DOI. ADS.

Morton, R.J., Verth, G., Jess, D.B., Kuridze, D., Ruderman, M.S., Mathioudakis, M., Erdélyi, R.: 2012, Observations of ubiquitous compressive waves in the Sun's chromosphere. *Nat. Commun.* **3**, 1315. DOI. ADS.

Nagata, S., Hara, H., Kano, R., Kobayashi, K., Sakao, T., Shimizu, T., Tsuneta, S., Yoshida, T., Gurman, J.B.: 2003, Spatial and temporal properties of hot and cool coronal loops. *Astrophys. J.* **590**, 1095. DOI. ADS.

Nakariakov, V.M., Verwichte, E.: 2005, Coronal waves and oscillations. *Living Rev. Sol. Phys.* **2**, 3. DOI. ADS.

Nakariakov, V.M., Verwichte, E., Berghmans, D., Robbrecht, E.: 2000, Slow magnetoacoustic waves in coronal loops. *Astron. Astrophys.* **362**, 1151. ADS.

Nakariakov, V.M., Zhong, S.H., Kolotkov, D.Y.D.Y., Meadowcroft, R.L., Zhong, Y., Yuan, D.: 2024, Diagnostics of the solar coronal plasmas by magnetohydrodynamic waves: magnetohydrodynamic seismology. *Rev. Mod. Plasma Phys.* **8**, 19. DOI. ADS.

Nightingale, R.W., Aschwanden, M.J., Hurlburd, N.E.: 1999, Time variability of EUV brightenings in coronal loops observed with TRACE. *Sol. Phys.* **190**, 249. DOI. ADS.

Ofman, L., Nakariakov, V.M., DeForest, C.E.: 1999, Slow magnetosonic waves in coronal plumes. *Astrophys. J.* **514**, 441. DOI. ADS.

Ofman, L., Nakariakov, V.M., Sehgal, N.: 2000, Dissipation of slow magnetosonic waves in coronal plumes. *Astrophys. J.* **533**, 1071. DOI. ADS.

Ofman, L., Wang, T.: 2002, Hot coronal loop oscillations observed by SUMER: slow magnetosonic wave damping by thermal conduction. *Astrophys. J.* **580**, L85. DOI. ADS.

Ofman, L., Romoli, M., Poletto, G., Noci, C., Kohl, G.L.: 1997, Ultraviolet coronagraph spectrometer observations of density fluctuations in the solar wind. *Astrophys. J. Lett.* **491**, L111. DOI. ADS.

Ofman, L., Romoli, M., Poletto, G., Noci, C., Kohl, G.L.: 2000, UVCS WLC observations of compressional waves in the south polar coronal hole. *Astrophys. J.* **529**, 592. DOI. ADS.

Okamoto, T.J., Tsuneta, S., Berger, T.E., Ichimoto, K., Katsukawa, Y., Lites, B.W., Nagata, S., Shibata, K., Shimizu, T., Shine, R.A., Suematsu, Y., Tarbell, T.D., Title, A.M.: 2007, Coronal transverse magnetohydrodynamic waves in a solar prominence. *Science* **318**, 1577. DOI. ADS.

Polyanin, A.D.: 2002, *Handbook of Linear Partial Differential Equations for Engineers and Scientists*, Chapman & Hall, London.

Priest, E.: 1982, *Solar Mangneto-Hydrodynamics, Geophysics and Astrophysics Monographs*, Kluver Academic Publishers.

Prudnikov, A.P., Brychkov, Y.A., Marichev, O.I.: 1992, *Integrals and Series*, CRC Press, Boca Raton.

Rudenko, O.V., Soluyan, S.I.: 2001, *Theoretical Foundation of Nonlinear Acoustics*, Consultant Bureau, New York.

Ruderman, M.S.: 2011a, Transverse oscillations of coronal loops with slowly changing density. *Sol. Phys.* **271**, 41. DOI. ADS.

Ruderman, M.S.: 2011b, Resonant damping of kink oscillations of cooling coronal magnetic loops. *Astron. Astrophys.* **534**, A78. DOI. ADS.

Ruderman, M.S.: 2013, Nonlinear damped standing slow waves in hot coronal magnetic loops. *Astron. Astrophys.* **553**, A23. DOI. ADS.

Ruderman, M.S.: 2019, *Fluid Dynamics and Linear Elasticity*, Springer, Switzerland.

Ruderman, M.S., Shukhobodskiy, A.A., Erdélyi, R.: 2017, Kink oscillations of cooling coronal loops with variable cross-section. *Astron. Astrophys.* **602**, A50. DOI. ADS.

Schrijver, C.J., Title, A.M., Berger, T.E., Fletcher, L., Hurlburt, N.E., Nightingale, R.W., Shine, R.A., Tarbell, T.D., Wolfson, J., Golub, L., Bookbinder, J.A., DeLuca, E.E., McMullen, R.A., Warren, H.P., Kankelborg, C.C., Handy, B.N., De Pontieui, B.: 1999, A new view of the solar outer atmosphere by the transition region and coronal explorer. *Sol. Phys.* **187**, 261. DOI. ADS.

Sigalotti, L.D.G., Mendoza-Briceño, C.A., Luna-Cardozo, M.: 2007, Dissipation of standing slow magnetoacoustic waves in hot coronal loops. *Sol. Phys.* **246**, 187. DOI. ADS.

Spitzer, L.J.: 1962, *Physics of Fully Ionazed Gases*, Wiley-Interscience, New York.

Taniuti, T., Wei, C.-C.: 1968, Reductive perturbation method in nonlinear wave propagation. I. *J. Phys. Soc. Jpn.* **24**, 941. DOI. ADS.

Taroyan, Y., Erdélyi, R., Wang, T.J., Bradshaw, S.J.: 2007, Forward modeling of hot loop oscillations observed by SUMER and SXT. *Astrophys. J. Lett.* **659**, L173. DOI. ADS.

Vaiana, G.S., Krieger, A.S., Timothy, A.F.: 1973, Identification and analysis of structures in the corona from X-ray photography. *Sol. Phys.* **32**, 81. DOI. ADS.

Verwichte, E., Haynes, M., Arber, T.D., Brady, C.S.: 2008, Damping of slow MHD coronal loop oscillations by shocks. *Astrophys. J.* **685**, 1286. DOI. ADS.

Viall, N.M., Klimchuk, J.A.: 2012, Evidence for widespread cooling in an active region observed with the SDO Atmospheric Imaging Assembly. *Astrophys. J.* **753**, 35. DOI. ADS.

Wang, T.J., Solanki, S.K., Innes, D.E., Curdt, W., Marsch, E.: 2003, Slow-mode standing waves observed by SUMER in hot coronal loops. *Astron. Astrophys.* **402**, L17. DOI. ADS.

Wang, T.J., Ofman, L., Yuan, D., Reale, F., Kolotkov, D.Y., Srivastava, A.K.: 2021, Slow-mode magnetoacoustic waves in coronal loops. *Space Sci. Rev.* **217**, 34. DOI. ADS.

Whitham, G.B.: 1974, *Linear and Non-linear Waves*, John Willey and Sons, New York.

Winebarger, A.R., Warren, H.P., Seaton, D.B.: 2003, Evolving active region loops observed with the transition region and coronal explorer. I. Observations. *Astrophys. J.* **593**, 1164. DOI. ADS.

Zaqarashvili, T.V., Erdélyi, R.: 2009, Oscillations and waves in solar spicules. *Space Sci. Rev.* **149**, 355. DOI. ADS.